AD-A049 679

NORTH CAROLINA UNIV AT CHAPEL HILL WILLIAM R KENAN JR--ETC F/G 7/4
CHEMICAL MODIFICATION OF CARBON ELECTRODES. X. ESCA AND AC VOLT--ETC(U)
JAN 78 R W MURRAY   N00014-76-C-0817
TR-3   NL

UNCLASSIFIED

| OF |
AD
A049 679

END
DATE
FILMED
3 -78
DDC

OFFICE OF NAVAL RESEARCH

Contract N00014-76C-0817

Task No. NR 359-623

TECHNICAL REPORT NO. 3

CHEMICALLY MODIFICATION OF CARBON ELECTRODES

by

Royce W. Murray

University of North Carolina
Kenan Laboratories of Chemistry
Chapel Hill, North Carolina 27514

January 1978

REPORT DOCUMENTATION PAGE

READ INSTRUCTIONS
BEFORE COMPLETING FORM

1. REPORT NUMBER	2. GOVT ACCESSION NO.	3. RECIPIENT'S CATALOG NUMBER
Technical Report No. 3		

4. TITLE (and Subtitle)

Chemical Modification of Carbon Electrodes.
X. ESCA and AC Voltammetry of Glassy
Carbon-Bound Tetra (aminophenyl)
porphyrins

5. TYPE OF REPORT & PERIOD COVERED

Interim rept,

6. PERFORMING ORG. REPORT NUMBER

7. AUTHOR(s)

Royce W. Murray

8. CONTRACT OR GRANT NUMBER(s)

N00014-76C-0817

9. PERFORMING ORGANIZATION NAME AND ADDRESS

Department of Chemistry
University of North Carolina
Chapel Hill, NC 27514

10. PROGRAM ELEMENT, PROJECT, TASK
AREA & WORK UNIT NUMBERS

NR 359-623

11. CONTROLLING OFFICE NAME AND ADDRESS

Office of Naval Research
Department of the Navy
Arlington, Virginia 22217

12. REPORT DATE

Jan 78

13. NUMBER OF PAGES

25p.

14. MONITORING AGENCY NAME & ADDRESS(if different from Controlling Office)

Office of Naval Research
ONR Branch Office
536 South Clark Street
Chicago, Illinois 60605

15. SECURITY CLASS. (of this report)

Unclassified

15a. DECLASSIFICATION/DOWNGRADING
SCHEDULE

16. DISTRIBUTION STATEMENT (of this Report)

Approved for Public Release, Distribution Unlimited

TR-3

17. DISTRIBUTION STATEMENT (of the abstract entered in Block 20, if different from Report)

18. SUPPLEMENTARY NOTES

Prepared for publication in **Journal of the American Chemical Society**

19. KEY WORDS (Continue on reverse side if necessary and identify by block number)

carbon electrode, ESCA, porphyrin, surface structure, cyclic voltammetry

20. ABSTRACT (Continue on reverse side if necessary and identify by block number)

ESCA data show that tetra(aminophenyl)porphyrin is bound to glassy carbon electrode surfaces by an average of two amide bonds. The bound porphyrin, its Co-metallated analog, and a nitroaromatic bound to the porphyrin via the dangling amine sites, exhibit electrochemical surface waves detected by cyclic, differential pulse and AC voltammetry. Axial coordination of immobilized porphyrin is demonstrated by sensitivity of the electrochemistry to added bases.

DD FORM 1 JAN 73 1473 EDITION OF 1 NOV 65 IS OBSOLETE

408 860

No. Copies   No. Copies

Office of Naval Research
Arlington, Virginia 22217
Attn: Code 472,   2

Office of Naval Research
Arlington, Virginia 22217
Attn: Code 102IP   6

ONR Branch Office
536 S. Clark Street
Chicago, Illinois 60605
Attn: Dr. George Sandoz   1

ONR Branch Office
715 Broadway
New York, New York 10003
Attn: Scientific Dept.   1

ONR Branch Office
1030 East Green Street
Pasadena, California 91106
Attn: Dr. R. J. Marcus   1

ONR Branch Office
760 Market Street, Rm. 447
San Francisco, California 94102
Attn: Dr. P. A. Miller   1

ONR Branch Office
495 Summer Street
Boston, Massachusetts 02210
Attn: Dr. L. H. Peebles   1

Director, Naval Research Laboratory
Washington, D.C. 20390
Attn: Library, Code 2029 (ONRL)   6
       Technical Info. Div.   1
       Code 6100, 6170   1

The Asst. Secretary of the Navy (R&D)
Department of the Navy
Room 4E736, Pentagon
Washington, D.C. 20350   1

Commander, Naval Air Systems Command
Department of the Navy
Washington, D.C. 20360
Attn: Code 310C (H. Rosenwasser)   1

Defense Documentation Center
Building 5, Cameron Station
Alexandria, Virginia 22314   12

U.S. Army Research Office
P.O. Box 12211
Research Triangle Park, North Carolina 27709
Attn: CRD-AA-IP

Commander
Naval Undersea Research & Development
Center
San Diego, California 92132
Attn: Technical Library, Code 133   1

Naval Weapons Center
China Lake, California 93555
Attn: Head, Chemistry Division   1

Naval Civil Engineering Laboratory
Port Hueneme, California 93041
Attn: Mr. W. S. Haynes   1

Professor O. Heinz
Department of Physics & Chemistry
Naval Postgraduate School
Monterey, California 93940

Dr. A. L. Slafkosky
Scientific Advisor
Commandant of the Marine Corps (Code RD-1)
Washington, D.C. 20380   1

Advanced Research Projects Agency
Materials Sciences Office
1400 Wilson Boulevard
Arlington, Virginia 22209
Attn: Dr. Stan Ruby   1

TECHNICAL REPORT DISTRIBUTION LIST

No. Copies

No. Copies

Dr. Paul Delahay
New York University
Department of Chemistry
New York, New York 10003   1

Dr. R. A. Osteryoung
Colorado State University
Department of Chemistry
Fort Collins, Colorado 80521   1

Dr. E. Yeager
Case Western Reserve University
Department of Chemistry
Cleveland, Ohio 41106   1

Dr. D. N. Bennion
University of California
Energy Kinetics Department
Los Angeles, California 90024   1

Dr. J. W. Kauffman
Northwestern University
Department of Materials Science
Evanston, Illinois 60201   1

Dr. R. A. Marcus
University of Illinois
Department of Chemistry
Urbana, Illinois 61801   1

Dr. M. Eisenberg
Electrochimica Corporation
2485 Charleston Road
Mountain View, California 94040   1

Dr. J. J. Auborn
GTE Laboratories, Inc.
40 Sylvan Road
Waltham, Massachusetts 02154   1

Dr. Adam Heller
Bell Telephone Laboratories
Murray Hill, New Jersey   1

Dr. T. Katan
Lockheed Missiles & Space Co., Inc.
P.O. Box 504
Sunnyvale, California 94088   1

Dr. R. A. Huggins
Stanford University
Department of Materials Science
   & Engineering
Stanford, California 94305   1

Dr. Joseph Singer, Code 302-1
NASA-Lewis
21000 Brookpark Road
Cleveland, Ohio 44135   1

Dr. B. Brummer
EIC Incorporated
Five Lee Street
Cambridge, Massachusetts 02139   1

Library
P. R. Mallory and Company, Inc.
P. O. Box 706
Indianapolis, Indiana 46206   1

Dr. P. J. Hendra
University of Southampton
Department of Chemistry
Southampton SO9 5NH
United Kingdom

Dr. Sam Perone
Purdue University
Department of Chemistry
West Lafayette, Indiana 47907   1

Dr. Royce W. Murray
University of North Carolina
Department of Chemistry
Chapel Hill, North Carolina 27514   1

Dr. J. Proud
GTE Laboratories Inc.
Waltham Research Center
40 Sylvan Road
Waltham, Massachusetts 02154   1

Mr. J. F. McCartney
Naval Undersea Center
Sensor and Information Technology Dept.
San Diego, California 92132   1

Chemically Modified Electrodes X. ESCA and AC Voltammetry
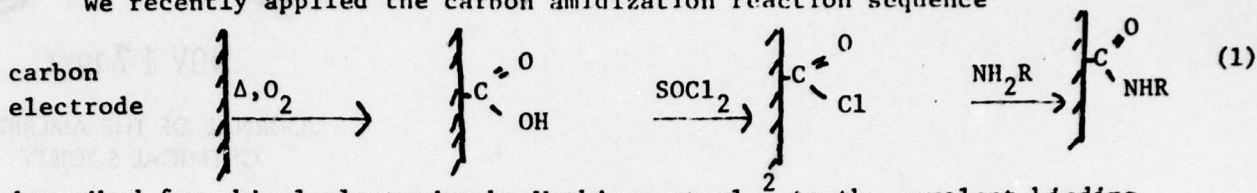of Glassy Carbon-Bound Tetra(aminophenyl)porphyrins

John C. Lennox[1] and Royce W. Murray[*]
Kenan Laboratories of Chemistry
University of North Carolina
Chapel Hill, N.C. 27514
RECEIVED NOV 17 1977

Abstract

ESCA data show that tetra(aminophenyl)porphyrin is bound to glassy

carbon electrode surfaces by an average of two amide bonds. The bound

porphyrin, its Co-metallated analog, and a nitroaromatic bound to the

porphyrin via the dangling amine sites, exhibit electrochemical surface

waves detected by cyclic, differential pulse and AC voltammetry. Axial coordination

of immobilized porphyrin is demonstrated by sensitivity of the electrochemistry

to added bases.

We recently applied the carbon amidization reaction sequence

$$\text{carbon electrode} \xrightarrow{\Delta, O_2} \overset{O}{\underset{OH}{C}} \xrightarrow{SOCl_2} \overset{O}{\underset{Cl}{C}} \xrightarrow{NH_2R} \overset{O}{\underset{NHR}{C}} \quad (1)$$

described for chiral electrodes by Watkins, et. al.[2] to the covalent binding

of tetra(aminophenyl)porphyrin to glassy carbon electrode surfaces[3]. The

thus immobilized porphyrin, designated C-/-T(NH$_2$)PP, is electrochemically

reactive, exhibiting reversible cyclic voltammetric waves in solutions devoid

of dissolved porphyrin, at potentials close to those of cyclic voltammograms

of dissolved T(NH$_2$)PP in conventional solutions. C-/-T(NH$_2$)PP electrode

surfaces can furthermore be metallated with Co(II), after which electro-

chemical reduction of CoT(NH$_2$)PP is observed. Electrochemical and ESCA

control experiments demonstrated[3] that the observed porphyrin immobilization,

under the circumstances of our experiments, depends on amide bonding as in

Reaction 1, as distinct from adsorption of porphyrin from aqueous solutions

onto carbon reported by Anson, et. al.[4,5]

Results of further experiments on glassy carbon-immobilized T(NH$_2$)PP

and CoT(NH$_2$)PP are presented in this paper. The number of amide bonds formed

between the tetra(aminophenyl)porphyrin and the carbon surface has been

determined by ESCA derivatization-analysis, and electrochemical effects of

axial coordination of immobilized CoT(NH$_2$)PP are observed. The excellent

sensitivity of phase selective AC voltammetry for surface redox processes

proved important in experiments on surfaces bearing both T(NH$_2$)PP and

CoT(NH$_2$)PP.

EXPERIMENTAL

Preparation and binding of tetra(m-aminophenyl)porphyrin, T(m-NH$_2$)PP, and tetra (p-aminophenyl)porphyrin, T(p-NH$_2$)PP, to glassy carbon was performed as detailed previously. Metallation was by warming with CoCl$_2$ in DMF or CH$_3$CN. The para- and ortho- isomers of mono-amino-tetraphenylporphyrin, M(NH$_2$)TPP, were generous gifts from C. M. Elliott (Stanford University). For investigation of amide binding, electrodes to which T(m-NH$_2$)PP had been bound were reacted with 3,5-dinitrobenzoyl chloride in toluene under gentle reflux for one hour. Relative areas of N 1s ESCA peaks observed on these electrodes were ascertained using a gaussian/lorentzian peak-fitting program designed specifically for ESCA applications[6]. $I_{amide}/I_{nitro} = 0.80$ on a standard material, 3,5-dinitrobenzanilide, and this correction factor was applied to the electrode results. ESCA spectra were obtained using a DuPont 650B spectrometer modified with an in-house designed microcomputer control and acquisition system.
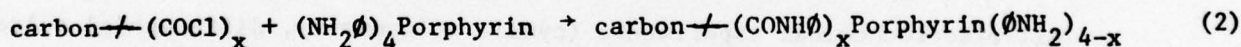
All electrochemical experiments (cyclic voltammetry, differential pulse voltammetry, AC voltammetry) employed a conventional non-aqueous cell, with Luggin (NaSCE) reference electrode probe, and a PAR Model 174 as a potentiostat. A simple modification to this instrument allowed setting the drop life (pulse repetition rate) at 0.1 - 0.5 seconds for differential pulse voltammetry. For AC voltammetry, signals were obtained from the output of the current transducer amplifier in order to bypass output buffers and filters which are present. AC measurements utilized a PAR HR-8 lock-in amplifier

-2-

for reference signal source and phase sensitive detection. Glassy carbon

electrodes were grade V10-50 from Atomergic Chemetals Corp. (Plainview, N.Y.),

cut as 2.7-3mm diameter, 4-5mm length cylinders. All electrochemical and

ESCA experiments are carried out on the cylinder ends, which are resurfaced

mirror-smooth with $\underline{1}$ micron diamond polishing compound after each use.

Solvents for electrochemistry were stored over molecular sieves (DMSO, CH_3CN)

or distilled freshly (DMF), and uniformly contained 0.1 $\underline{M}$ $Et_4N^+ClO_4^-$
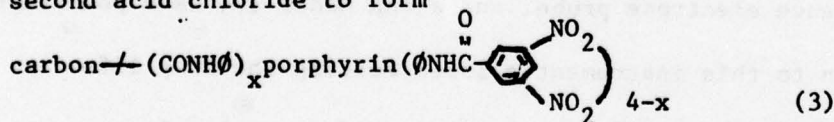
electrolyte.

RESULTS AND DISCUSSION

Number of amide bonds. Previous experiments[3] showed that the binding of

$T(NH_2)PP$ to glassy carbon is associated with the presence of the amine groups

on the porphyrin moiety. Formation of four amide bonds was thought unlikely

on steric grounds. Analysis of the number of bonds which do form is an

important part of a stereochemical picture of the modified surface.

Representing the amidization reaction as

$$\text{carbon} \mathord{-}\!\!\!| \mathord{-} (COCl)_x + (NH_2\emptyset)_4 \text{Porphyrin} \rightarrow \text{carbon} \mathord{-}\!\!\!| \mathord{-} (CONH\emptyset)_x \text{Porphyrin}(\emptyset NH_2)_{4-x} \quad (2)$$

the residual amine sites can be determined by derivatization with a

second acid chloride to form

$$\text{carbon} \mathord{-}\!\!\!| \mathord{-} (CONH\emptyset)_x \text{porphyrin}(\emptyset NHC \overset{O}{\overset{\|}{-}} \underset{NO_2}{\overset{NO_2}{\bigcirc}})_{4-x} \quad (3)$$

The N 1s ESCA peaks of the amide and porphyrin nitrogens (400 e.v.) are

unresolved from one another but are well resolved from nitro nitrogen

(407 e.v.) (Figure 1). The relative areas of the two N 1s peaks

provide an estimate of the percentage free amine remaining after Reaction 2.

In two determinations using four electrode specimens each, the percentage

free amine for immobilized $T(\underline{m}\text{-}NH_2)PP$ was 45±7% and 50±13% (2σ). No

-3-

correction was applied to the 400 e.v. peak for a small nitrogen blank

present on freshly polished electrodes. Unmodified control electrodes

reacted with 3,5-dinitrobenzoyl chloride exhibit no significant 407 e.v.

(nitro) band; stable esters do not form under the conditions employed.

The free amine result indicates that $\underline{x} = 2$ in Reaction 2, e.g., on

the average, two of the four amines of $T(\underline{m}-NH_2)PP$ become bound to the carbon

electrode surface by an amide linkage. The distribution of $\underline{mono}$-, $\underline{bis}$-,

and $\underline{tris}$-bonded $T(\underline{m}-NH_2)PP$ which forms this average is unknown, and judging

from the data scatter may vary somewhat from electrode to electrode. A

predominance of $\underline{bis}$-bonded $T(NH_2)PP$ is, however, readily rationalized if it

is assumed that the surface acid chloride site density does not greatly

exceed the amine site "density" of the $T(\underline{m}-NH_2)PP$. Thus the three amine

groups on a freshly $\underline{mono}$-bonded, freely rotating $T(\underline{m}-NH_2)PP$ have a much

higher probability of encounter and reaction with an appropriately located

second acid chloride site than will the two amine groups remaining on the

ensuing, motionally restricted, α,β or α,γ $\underline{bis}$-bonded species. That is, the

probability of good steric register of two amine-acid chloride pairs is

greater than that of three.

Further insight into the porphyrin surface bonding awaits results of

experiments on the average surface acid chloride spacing and with appropriate

diaminotetraphenyl-porphyrin isomers.

Electrochemical observation of surface waves. Cyclic voltammetry is readily

applied to detection of chemisorbed[4,5,7,8] or synthetically linked[11-16] surface redox

couples at high coverage or low background, and presently is the method of choice for

systems of brief lifetime. For accurate measurements of formal potentials

and ΔE_{peak} values of surface waves, especially at low sweep rates, and for

characterization of surfaces at low coverages or which exhibit multiple

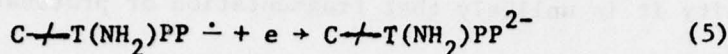redox processes, however, the quality of information from cyclic voltammetry
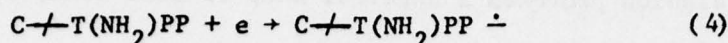
Fig. 2   can be poor (Figure 2, Curve A). An alternative experiment for surface studies,

differential pulse voltammetry, was introduced by Anson, et. al.[4,5] via a

clever manipulation of uncompensated cell resistance[9]. Figure 2, Curve B

illustrates the efficacy of this experiment on an electrode bearing a mixed

array of T($\underline{m}$-NH$_2$)PP and CoT($\underline{m}$-NH$_2$)PP sites.

       Phase selective AC voltammetry also promotes high sensitivity to surface

Fig. 3   redox events, (Figure 3). Residual, unmetallated T($\underline{m}$-NH$_2$)PP is undetectable

in the Curve A cyclic voltammogram, but is discerned in the AC experiment

(Curve B) at a coverage estimated at $\leq$ 2x10^{-12} mole/cm.^{2}. Both differential

pulse and AC voltammetries detect the electrode surface capacitance

dispersion which occurs at potentials for electron transfer reactions of

immobilized redox couples[10]. Both methods require modest potential sweep

rates (1-10 mv./sec.) to avoid E_{peak} shifts and demand stable (or replenished[5])

surface redox systems for prolonged observations.

C $\overline{+}$ TPP Electrodes. In DMSO, four reduction waves can be observed at

Table 1   C $\overline{+}$ T($\underline{m}$-NH$_2$)PP electrodes (Table 1, entry 1), two (Waves I) with potentials

(-1.08, -1.50) closely matching those at which dissolved TPP is reduced to

radical anion and dianion, and two (Waves II) with low and variable amplitude

observable only in differential pulse and AC voltammetry (Figure 3) responses.

-5-

We interpret Waves I in DMSO and Waves II in CH_3CN as

$$C\!\!-\!\!\!\!+\!\!\!\!-\!T(NH_2)PP + e \rightarrow C\!\!-\!\!\!\!+\!\!\!\!-\!T(NH_2)PP \overset{\cdot}{-} \qquad (4)$$

$$C\!\!-\!\!\!\!+\!\!\!\!-\!T(NH_2)PP \overset{\cdot}{-} + e \rightarrow C\!\!-\!\!\!\!+\!\!\!\!-\!T(NH_2)PP^{2-} \qquad (5)$$

The potentials for reactions 4 and 5 are shifted by -0.24 and -0.33 volts in CH_3CN as compared to DMSO, a large solvent effect. Acetonitrile is a poor solvating medium for porphyrins, and the large shift in potential can be attributed to solvation factors, or, more plausibly, to a reactant-stabilizing interaction of the bound porphyrin system with the carbon surface which is promoted by the poor solvating efficacy of the CH_3CN medium. In view of the fact that the potential shift occurs for both $T(NH_2)PP$ and $M(NH_2)PP$, and potentials for bound $CoT(NH_2)PP$ in contrast exhibit little dependency on solvent (Table I, entries 4,10,12), it is further likely that the surface-porphyrin interaction involves the central ring of the bound porphyrin.

In DMSO solvent, reversal of the direction of potential scan yields pseudocapacitance peaks for Waves I and II which are similar in amplitude and E_{peak} on cathodic and anodic-going scans. The same result is obtained in CH_3CN if scan reversal occurs (immediately or with a 60 sec constant potential pause) after the radical anion-producing -1.3v wave
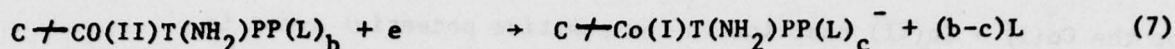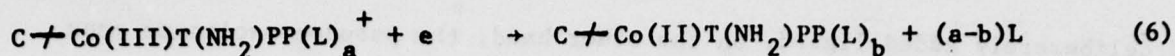
Fig. 4   (Figure 4, Curve B). Extension of the potential cycle to include the second, dianion wave, however, produces an attenuated radical anion reoxidation peak and a new wave at -0.40 (Figure 4, Curve A). No effect is seen on the pseudocapacitance peak during which the dianion is oxidized, and the overall process is reversible, e.g., a subsequent cyclic AC

-6-

voltammogram quantitatively repeats this pattern (Curve C). Clearly production of the dianion provokes a chemical step of some kind; from its overall reversibility it is unlikely that fragmentation or protonation of the perimeter porphyrin structure has occurred. Again involvement of the central ring is most plausible. It is possible that a portion of the porphyrins are bound in such a way that the central nitrogen base sites fall in register with a surface carboxylic acid or hydroxylic site, and in CH_3CN a stabilizing, reversible proton transfer from this site to the ring nitrogen occurs (e.g. $HT(NH_2)PP^-$).

Interpretation of the small population of species reacting in Waves II in DMSO and in Waves I in CH_3CN is unclear. These waves decay more rapidly than the main Reaction 4,5 waves in both solvents (compare Curves A, C, Figure 4). It is possible that Waves II in DMSO represent sites for which a surface-porphyrin interaction occurs akin to that proposed to occur for the majority of bound porphyrin in CH_3CN. Experiments in which $C\!\!-\!\!\!/\!\!-T(NH_2)PP$ electrodes are transferred between cells containing DMSO and CH_3CN solvent show moderately slow (~30 minutes) equilibration in the new solvent through slow changes in positions and relative amplitudes of Waves I and II.

Mixed $C\!\!-\!\!\!/\!\!-CoT(NH_2)PP$, $T(NH_2)PP$ electrodes. Metallation reactions carried out in CH_3CN leave a residue of bound but unmetallated $T(NH_2)PP$ whose electrochemistry serves as a convenient reference for solvent and axial ligand studies on the bound $CoT(NH_2)PP$. Figures 2 and 3 illustrate such mixed electrodes. Potentials of the two surface waves which appear upon cobalt metallation agree quite closely with those observed by Truxillo and Davis[17] for dissolved CoTPP complexes, and the +0.1 and -0.8 v. surface waves

-7-

can be identified respectively with the reactions

$$C + Co(III)T(NH_2)PP(L)_a^+ + e \rightarrow C + Co(II)T(NH_2)PP(L)_b + (a-b)L \quad (6)$$

$$C + CO(II)T(NH_2)PP(L)_b + e \rightarrow C + Co(I)T(NH_2)PP(L)_c^- + (b-c)L \quad (7)$$

Potentials for Reactions 4,5 and 6,7 are little if any affected by neighbor

metallated and unmetallated sites, respectively. The potential for Reaction 7

is relatively insensitive to solvent, but both it and (more strongly) Reaction

6 are shifted by added bases such as pyridine or methyl imidazole (Table I,

entries 4-6, 10-11, 12-14). The difference in Reaction 6 and 7 potentials is

0.73 ± 0.01 v for added pyridine and 0.51 ± 0.02 for methyl imidazole, independent

of solvent. The Reaction 6-7 potential difference with pyridine agrees with

that reported by Davis[17] for solutions of Co(TPP) containing added pyridine.

The shifts in Co porphyrin redox potentials with added ligand are

clearly associated with axial coordination of the metal center, and their

mere existance shows that at least one and possibly both axial sites on

immobilized $C + CoT(NH_2)PP$ are available for coordination. The magnitude

of the shifts likewise suggests that (a-b) and (b-c) in Reactions 6 and 7

are not altered from that in solution, although, thorough potential-ligand

concentration data are needed to be quantitative on this point.

Fig. 5 Cyclic AC voltammetry is again revealing. In CH_3CN solvent with added

methyl imidazole (Figure 5, Curve B), and in DMSO and DMF solvents with or

without added ligand, cyclical, slow potential sweep AC voltammetry of

$C + CoT(NH_2)PP$ is approximately the same on negative and positive-going

sweeps. (Some scatter using wide potential sweep ranges is attributed

to hysteresis in the background signals.) In CH_3CN, in the absence

-8-

of deliberately added ligand, on the other hand, the pseudocapacitance peak

for the Co(I) → Co(II) reaction in the positive potential sweep is

2-3 x larger in amplitude, and narrower in peak width, than that for the

Co(II) → Co(I) reaction (Figure 5, Curve A). This effect is more pronounced

at faster sweep rates (compare Curves C and D). ΔE_{peak} is larger in CH_3CN

than usual in DMSO. In conventional cyclic voltammetry on electrodes with

sufficiently high coverage, a sharper (thus seemingly larger) anodic wave

can be seen (Curve E). The amplitude effect in the cyclic AC voltammetry

primarily reflects the cathodic-anodic peakwidth difference; the method is

more sensitive to surface wave peakwidth than cyclic voltammetry, as is

differential pulse voltammetry[5].

The peakwidth and scan rate results in CH_3CN suggest a rather slow

change in cobalt axial coordination following Reaction 7 in this solvent.

Adventituous water, chloride, or an appropriate, underlying carbon surface

functionality constitute possible ligands; whichever is involved is recoverable

following reoxidation of C─╂─Co(I)T(NH$_2$)PP since the cyclic AC voltammograms

are repeatable. Such analogous coordination changes as may occur in the

presence of ligand or in DMSO solvent evidently are much more rapid, and

peakwidth hysteresis is not seen.

The underlying basis of differing peakwidths for the Co(II) → Co(I) and

Co(I) → Co(II) reactions, as a consequence of the supposed coordination

change, is of some interest. If interpreted in terms of non-ideality

interaction parameters;[5,8,18] it follows from these results that such

parameters can be quite structure-sensitive. An alternate explanation

invokes actual structural non-uniformity (and thus

a band-broadening spectrum of surface couple formal potentials E°') throughout

the surface ensemble. The extent of this chemical diversity could well

depend on oxidation state. If the structural readjustments following electron

transfer are slow, both structural heterogeniety and non-ideality parameter views

anticipate a peakwidth difference between the cathodic and anodic reaction.

As a formalism, of course, structural non-uniformity can be accomodated

within the framework of non-ideality parameters, as involvement of neighbor-

neighbor site <u>interactions</u> is not required for non-ideality. We have

observed cathodic-anodic peakwidth differences on other occassions, for

instance the metal oxide electrode immobilized[13,19] $-CO\phi(NO_2)\frac{\cdot}{2} \rightleftarrows -CO\phi(NO_2)_2^{2-}$

and $-$tetrathiafulvaline$^+ \rightleftarrows -$tetrathiafulvaline^{2+} reactions[20]. In these cases

sweep rate and structural change effects have not been identified.

A comparison of the waves for Reactions 6 and 7 as seen in Figures 2,

and 3 (Curves C, D) shows that irrespective of solvent,

presence of added ligand, or method employed, the Co(III) $\rightleftarrows$ Co(II) porphyrin

wave is broader and of substantially lower amplitude than the Co(II) $\rightleftarrows$ Co(I)

process. The amplitude difference is doubtless in part due to the peakwidth

sensitivity of differential pulse and AC voltammetry; interaction and/or

chemical heterogeniety effects could well differ in the two reactions. In

the absence of a quantitative treatment of the amplitude-peakwidth relation,

however, we should not exclude a possible difference in charge transfer

kinetics, since charge transfer rates for dissolved CoTPP complexes are

fairly slow, and moreso for the Co(III) $\rightleftarrows$ step[17].

-10-

Finally, we previously[3] noted that electrochemical waves on C—T(NH$_2$)PP and C—CoT(NH$_2$)PP electrodes persist for many cycles. Further experience has shown that stability of the surface redox couples varies somewhat from electrode to electrode, but in general C—CoT(NH$_2$)PP electrochemistry is very stable, and that of C—T(NH$_2$)PP moderately so. Half-lives of 300-1200 seconds (reduced state) have been observed for C—T(NH$_2$)PP electrodes. One C—CoT(NH$_2$)PP electrode was reduced (Co(I) state) in DMSO for 10^4 seconds, then cycled 500 times in Reaction 7. The re-examined Reaction 7 AC voltammetric wave amplitude was (within ± 10%) <u>unchanged</u> from its original value. Such stability of a ≤ monomolecular layer is remarkable. C—CoT(NH$_2$)PP electrodes have on several occassions been rinsed following an afternoon's experimentation, stored air-dry or under solvent, and successfully re-used on the next day. Potential scans into the cathodic carbon background rapidly degrade the redox ensembles.

<u>C—T(NH$_2$)PP-CO∅(NO$_2$)$_2$ electrodes.</u> Several specimens prepared during the amide linkage analysis of Figure 1 were examined as electrodes in DMF. Reduction waves at -0.7, -0.9, -1.2, and -1.6 were observed using AC voltammetry; the first two waves decayed rapidly in comparison to the second two. The first and third potentials are approximately those of otherwise immobilized[12,13] —CO∅(NO$_2$)$_2$; the other two approximate those seen on C—T(NH$_2$)PP electrodes. It appears that the electroactive —CO∅(NO$_2$)$_2$ group has been immobilized on carbon electrodes using in effect the T(NH$_2$)PP as a bridging reagent. This is a provocative observation the possibilities of which for chemically modifying carbon are being further explored.

-11-

DISCUSSION

These results continue to support the hypothesis that to a first approximation electrochemistry of an electrode-immobilized chemical can be anticipated from that of its dissolved counterpart. Exceptions arise, and in the present case they are provoked by use of a poorly solvating medium. It is of interest to note in this connection that solubility of a redox couple, once immobilized on the chemically modified electrode surface, is no bar to experimentation, but observed electrochemical properties may then reflect specific surface effects.

Two aspects of detailed structure of carbon-bonded tetra(aminophenyl)porphyrin were revealed in that two amide bonds form, on the average, with the carbon, and that axial sites in bonded $CoT(NH_2)PP$ are open for coordinative attack. These two features are consistent with the hypothesis that stable chemically modified surfaces are amenable to predictive electrocatalysis[21].

Acknowledgement

REFERENCES

(1.) Present address University of Arkansas, Fayetteville, Ark.

(2.) B. F. Watkins, J. R. Behling, E. Kariv, and L. L. Miller, J. Amer. Chem. Soc., 97, 3549 (1975).

(3.) J. C. Lennox and R. W. Murray, J. Electroanal. Chem., 78, 395 (1977).

(4.) A. P. Brown, C. Koval, and F. C. Anson, J. Electroanal. Chem., 72, 379 (1976).

(5.) A. P. Brown and F. C. Anson, Anal. Chem., (1977).

(6.) David N. Smith, University of North Carolina, unpublished results, 1976.

(7.) R. F. Lane and A. T. Hubbard, J. Phys. Chem., 77, 1401, 1444 (1973).

(8.) E. Laviron, J. Electroanal. Chem., 47, 2260 (1975).

(9.) We have confirmed the uncompensated cell resistance dependency described by Anson[5], and also observe additional sensitivity enhancement at shortened pulses (e.g. 0.1 sec/pulse) and via the peak current-pulse amplitude (5-100 mv.) proportionality.

(10.) Representing the faradaic pseudocapacitance as C_f, and using a fast charge transfer equivalent circuit model[5], the AC response to $\Delta E \sin(\omega t)$ excitation is

$$i_{ac} = \frac{\Delta E \omega \, (C_{d1} + C_f)}{[1 + \omega^2 R_u^2 (C_{d1} + C_f)^2]^{1/2}} \, \sin(\omega t + \phi)$$

where $\tan \phi = [\omega R_u (C_{d1} + C_f)]^{-1}$. When $C_f \gg C_{d1}$, $\omega R_u C_f < 1$, and C_f invariant over ΔE, (so $\phi = 90°$); $i_{ac} = \Lambda F \omega C_f$, and $(i_{ac})_{max}$ occurs at $(C_f)_{max}$ which is at $E°'$.

(11.) P. R. Moses and R. W. Murray, J. Amer. Chem. Soc., 98, 7435 (1976).

(12.) P. R. Moses and R. W. Murray, J. Electroanal. Chem., 77, 393 (1977).

(13.) J. R. Lenhard and R. W. Murray, J. Electroanal. Chem., 78, 195 (1977).

(14.)   A. Diaz, J. Amer. Chem. Soc., _99_, 5838 (1977).

(15.)   J. F. Evans and T. Kuwana, Anal. Chem., _49_, 1632 (1977).

(16.)   M. S. Wrighton, private communication, 1977.

(17.)   L. A. Truxillo and D. G. Davis, Anal. Chem., _37_, 2260 (1975).

(18.)   B. E. Conway and E. Gileadi, Trans. Far. Soc., _58_, 2493 (1962).

(19.)   J. R. Lenhard, unpublished results, 1977.

(20.)   P. R. Moses, unpublished results, 1977.

(21.)   J. F. Evans, T. Kuwana, M. T. Henne, G. P. Royer, J. Electroanal.
        Chem., _80_, 409 (1977).

Figure Legends

Figure 1. N 1s ESCA spectrum of glassy carbon electrode modified to bear

structure shown in Reaction 3.

Figure 2. Cyclic voltammetry (Curve A, 0.1v./sec.) and differential pulse

voltammetry (Curve B, scan rate 2 mV/sec., pulse rate 125 msec./pulse,

10 mV. pulse amplitude) for a carbon—/—T(p-NH$_2$)PP electrode partially

Co-metallated, in DMF solvent with added pyridine.

Figure 3. Cyclic voltammetry of a low coverage carbon—/—CoT($\underline{m}$-NH$_2$)PP

electrode at 0.1 v./sec. (Curve A). AC voltammetry of assorted

electrodes at 10 mV/sec potential sweep rate, 5 mV amplitude 40 Hz

sinusoidal excitation, 90° phase detection; Curve B: same electrode as

Curve A; Curve C: mixed carbon—/—CoT($\underline{m}$-NH$_2$)PP,T($\underline{m}$-NH$_2$)PP electrode;

Curve D: same electrode as Curve C with methyl imidazole added to

solvent; Curves E and F: carbon—/—T($\underline{m}$-NH$_2$)PP electrodes; Curve G:

carbon—/—M($\underline{p}$-NH$_2$)TPP electrode; Curve H: carbon—/—M($\underline{o}$-NH$_2$)TPP

electrode. All in DMSO solvent. Curves offset for clarity.

Figure 4. Cyclic AC voltammetry of carbon—/—T($\underline{m}$-NH$_2$)PP in CH$_3$CN solvent.

5 mV/sec potential sweep rate, 5 mV. amplitude 40 Hz sinusoidal

excitation, 90° phase detection. Curve A: Initial cyclic scan,

immediate scan reversal; Curve B: pause at -1.50 volt 60 seconds

before reversal; Curve C: repeat of Curve A after extensive cycling.

Figure 5. Cyclic AC voltammetry of mixed carbon—/—CoT($\underline{p}$-NH$_2$)PP,T($\underline{p}$-NH$_2$)PP

electrode in CH$_3$CN solvent; 5 mV. amplitude 40 Hz sinusoidal excitation;

90° phase detection. Curve A: 5 mV/sec potential sweep rate;

Curve B: 5 mV/sec potential sweep rate and added methyl imidazole;

Curve C: 2 mV/sec potential sweep rate; Curve D: 20 mV/sec potential

sweep rate; Curve E: cyclic voltammetry of carbon—/—CoT($\underline{p}$-NH$_2$)PP

electrode at 0.10 v/sec., voltage axis not shown.

Table I Reduction Potentials for Tetraphenylporphyrins Bound to Glassy Carbon

Entry	Solvent[a]	Electrode[b]	E_{peak}^{c} vs NaSCE			
			Co(3/2)TPP	Co(2/1)TPP	TPP(0/-1)	TPP(-1/-2)
1	DMSO	T(m-NH$_2$)PP	-	-	-1.08 (-1.14)	-1.50 (-1.70)
2	DMSO	M(p-NH$_2$)TPP	-	-	-1.06 -1.14	-1.45 -1.63
3	DMSO	M(o-NH$_2$)TPP	-	-	-1.15	-1.45 -1.63
4	DMSO	T(m-NH$_2$)PP+Co	+0.10	-0.86	-1.10	-1.51
5	DMSO+Py	T(m-NH$_2$)PP+Co	-0.18	-0.91	-1.10	-1.49
6	DMSO+MeIm	T(m-NH$_2$)PP+Co	-0.39	-0.92	-1.10	-1.49
7	CH$_3$CN	T(m-NH$_2$)PP	-	-	-1.32	(-1.60) -1.83
8	CH$_3$CN	M(p-NH$_2$)TPP	-	-	(-1.16) -1.31	(-1.52) -1.76
9	CH$_3$CN	M(o-NH$_2$)TPP	-	-	-1.36	-1.76
10	CH$_3$CN	T(p-NH$_2$)PP+Co	n.obs.	-0.89	-1.37	-1.84
11	CH$_3$CN+MeIm	T(p-NH$_2$)PP+Co	-0.54	-1.03	-1.36	(-1.56) -1.84
12	DMF	T(p-NH$_2$)PP+Co	+0.06	-0.83	-1.14	-1.54
13	DMF+Py	T(p-NH$_2$)PP+Co	-0.18	-0.90	-1.14	-1.54
14	DMF+MeIm	T(p-NH$_2$)PP+Co	-0.41	-0.95	-1.14	-1.54

(a.) Py= pyridine, MeIm= methyl imidazole. (b.) T(m-NH$_2$)PP+Co signifies an incompletely metallated electrode which exhibits electrochemistry of both T(m-NH$_2$)PP and CoT(m-NH$_2$)PP. (c.) Data primarily from AC voltammetry cathodic-going scan, at potential sweep rate $\leq$ 10 mV/sec. Data in ( ) represent low intensity waves observed as shoulders or small peaks.

A(S=2 μa)

B(S=50 na)

S

D(S=200 na)

C(S=200 na)

E(S=400 na)

F(S=400 na)

G(S=100 na)

H(S=200 na)

I II

0   -1.0   -2.0

E vs Na SCE

A.

B.

C.

E vs NaSCE

0

-2.0

0

-2.0

0

-2.0

1 μa